

Experimental validation of metal powders deposition systems through additive manufacturing technology SLM

Summary of dissertation for the degree of Master in Materials Engineering

Authors¹

Frederico Mourato Freitas Malacho

¹Instituto Superior Técnico, Universidade Técnica de Lisboa, Portugal

fredericomalacho@gmail.com

ABSTRACT

Selective Laser Melting (SLM), is a manufacture technology that brought a big impact to the manufacture industry, because it allowed the reduction of production costs and time, mainly in part development when compared with casting technique.

SLM equipment is used nowadays, in small part production series, with a powder table size in average of 250mm*250mm.

The challenge with SLM technology begun, when these equipments achieved high standards quality. Manufacture companies started to use these equipments to reduced manufacture costs and to produce pieces with higher level of customisation.

With that, ADIRA Metal – Forming Solutions consider essential to design and validate a new experimental SLM equipment with higher working dimensions (1m³).

To validate the experimental equipment it was produced specimens and performed tests to evaluate the material and mechanical properties and compare it to specimens produced with commercial equipments and the theoretical values for a casted part.

Keywords

SLM, Process Parameters, Density, Porosities, Energy Input, Hatch Space, Vector Size, Hardness, Mechanical Behavior.

1. INTRODUCTION

Selective Laser Melting is an additive manufacture technique, that allows part production from from a three-dimensional computer file (3D-CAD).

SLM presents advantages over other metal additive manufacturing techniques, as higher dimensional accuracy, part complexity and the different materials that can be used.

The current SLM equipments presents low production rates, so the market for this method is components with high geometric complexity, that is typically very expensive and time consuming to manufacture from cast and machining techniques.

The new developments with this technique have been the increment in size and production rate.

For that, is essential to understand the relationship between the different technique parameters to be able to maximize the production rate without losing part quality.

This thesis have two objectives, the first is to understand the relation between process parameters and the second is to develop and validate a new SLM Equipment, by testing specimens produced by this experimental equipment (Add Creator, from Adira Metal-Forming Solutions, SA) with specimens manufactured by a commercial SLM equipment (M1 Cusing, by Concept Laser) and the theoretical values for 316L casted parts.

The Concept Laser equipment was used for studying the mechanical and metallurgical properties of already commercialized products. The Adira equipment, being under development, needs to adjust the process parameters to ensure the part quality doesn't get affected.

In State of Art chapter, is presented different additive techniques and the introduction to the SLM technique, including applications and the process that supports the technique. By the end of this chapter is yet possible, to see some studies that relates, different process parameters with the mechanical properties.

The methodology chapter, describes the tests applied and the SLM equipments, and the fourth chapter presents the experimental work and the obtain results.

According to research perform by Lavery et.al.[1] it is possible to obtain SLM samples with porosity content lower than 1 % in a range of energy input between 80 J/mm³ and 130 J/mm³. For this thesis it was used an exploration approach, to try to magnify the window with lower porosity content (in a range of 75 J/mm³ and 120 J/mm³) developed by Lavery et.al.[1] as can be seen in the Figure 1.

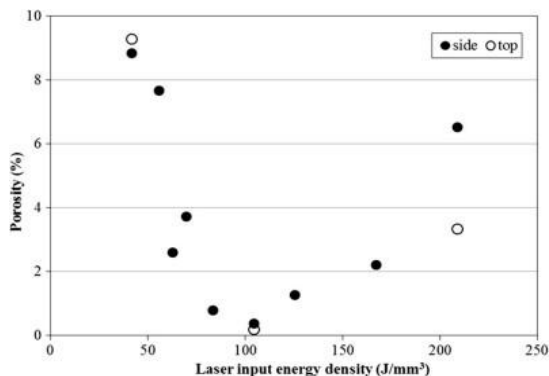


Figure 1 - Porosity versus laser energy density for builds, data points are measured values of porosity from optical microscopic images on one of the sides face (black circles) and top face (white circles) of the cubes which is build direction [1]

Knowing that, the energy input can be obtained by Equation 1, it can be seen that, it is possible to change the energy input value, just by changing the hatch space and vector size, keeping all the other variables constant.

$$Q = \frac{\text{Laser Power} * \left(\frac{\text{Exposure Time}}{\text{Hatch Space} + \text{Vector Length}} \right)}{\text{Layer Thickness}} \left(\frac{\text{J}}{\text{mm}^3} \right)$$

Equation 1

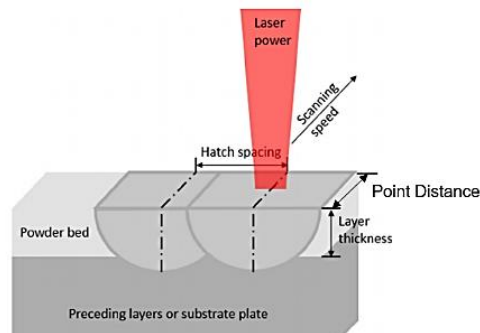


Figure 2 - Laser exposure. Process parameters: hatch Spacing or hatch distance; layer thickness, exposure time and point distance

The variables in the Equation 1 are explained bellow:

- Q – Energy input that is delivery to a volume unit;
- Exposure Time – Time period that a powder volume unit is exposed to the laser energy;
- Hatch space – Distance between welding seams;
- Point Distance (or Vector Length) – Distance that the laser goes without stop.

2. Method

In order to see the influence from energy input, hatch space and vector size in the specimen density and mechanical properties it was chosen to manufacture specimens with energy input values between 65 J/mm³ and 135 J/mm³, because accordingly with the Figure 1, is located in this region the energy input value that delivers the minimum porosity content.

Specimen Group	Energy Density J/mm ³	Laser Power (W)	Hatch Spacing (μm)	Vector size (mm)	Atmosphere
1	67,50	270	0,10	1	Argon
2	67,50	270	0,10	1	Nitrogen
3	67,50	270	0,10	5	Argon
4	67,50	270	0,10	5	Nitrogen
5	67,50	270	0,10	10	Argon
6	67,50	270	0,10	10	Nitrogen
7	67,50	270	0,10	15	Argon
8	67,50	270	0,10	15	Nitrogen
9	76,56	245	0,08	15	Argon
10	84,38	270	0,08	15	Argon
11	84,38	270	0,08	15	Nitrogen
12	135,00	270	0,05	10	Argon
13	135,00	270	0,05	10	Nitrogen
14	135,00	270	0,05	15	Argon
15	135,00	270	0,05	15	Nitrogen

Table 1 - Specimen group with different set parameters

To allow the material and mechanical specimen characterization it was perform the follow techniques:

- Scanning Electron Microscopy (SEM) - Identify the Solidification Structure;
- Magnetic Permeability - Identify phases with different impedances;
- Metallography - Metallurgical Characterization;
- Induced Chain Testing - Internal quality assessment;
- Density Tests - Check internal porosity;
- Hardness Tests - Evaluate through the hardness results, the phases present;
- Compressive and Tensile Testing - Mechanical Properties Evaluation;

3. Results and Discussion

The specimens manufactured by the commercial equipment, presented some defects at the surface, such as burrs and warps mainly from residual stress in the production phase, due thermal expansion effect, and a laser misalignment in a certain height (Z axis), leading to, in certain time, the laser started to melt an adjacent powder layer. This laser scanning error, although the problem in the visual appearance, didn't have influence in the specimen after machining the samples surfaces.

Both equipment (commercial and experimental) presented specimens with oxidized surfaces. This oxidation is present at final layer and it is believed, to have origin in the oxygen that is entrapped between the powder particle in the powder table.

To evaluate the presence of superficial and sub – superficial defects, as cracks, inclusions or porous it was performed induced current test in specimen produced by each equipment.

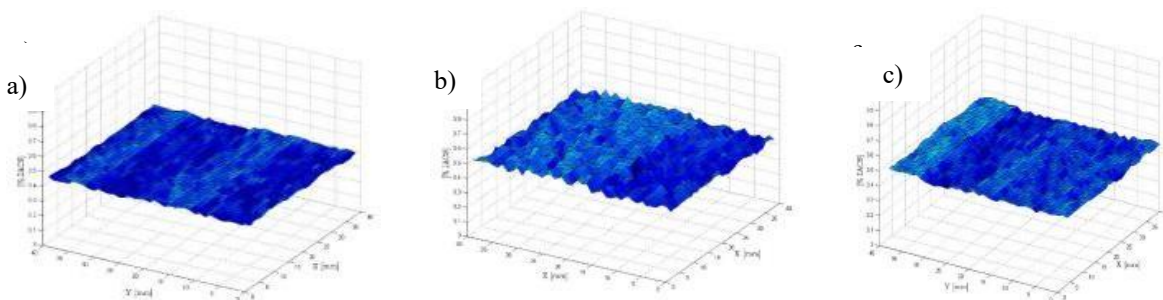


Figure 3 – 3D Representation from Commercial equipment specimens, in the electric conductivity in the face perpendicular to the axis: a) X, b) Y, c) Z

From the Figure 3 is possible to see a continuous profile with electric conductivity varying from 3.4 - 3.6 %IACS what shows some degree of homogeneity in the microstructure in all the specimens produced by the commercial equipment.

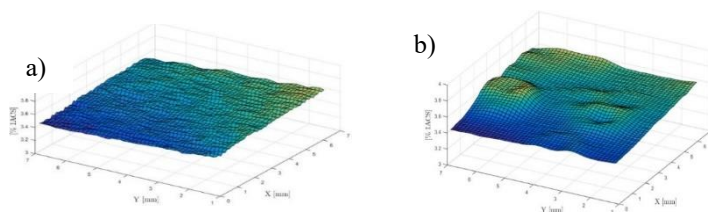


Figure 4 - 3D Representation from the Experimental equipment specimens

Figure 4 a) presents a constant electrical conductivity field, what shows absence of defects in the sample, although

Figure 4 b) presents some defects in the periphery region. With Figure 5 is possible to see that, the defects detected in the induced current test comes from the porous located at the specimen periphery.

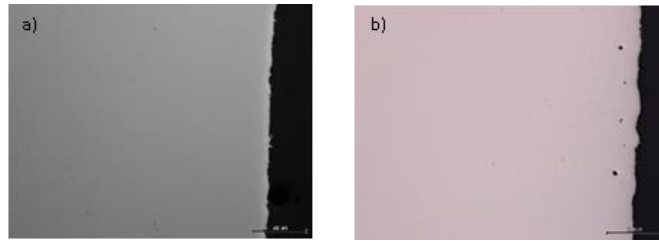


Figure 5 - Microscopic images from the experimental specimen under induce current test

Hardness Tests - Evaluate through the hardness results, the phases present;

It was performed hardness tests in the 15 specimen group, to evaluate the metallurgical phases and the influence in microstructure.

Specimen Group	Energy Density J/mm ³	Hatch Spacing (μm)	Vector size (mm)	Atmosphere	Hardness (Hv)	Standard Deviation Hardness (Hv)
1	67,5	0,1	1	Argon	211,2	9,9
2	67,5	0,1	1	Nitrogen	201,3	8,3
3	67,5	0,1	5	Argon	208,6	10,7
4	67,5	0,1	5	Nitrogen	206	7,6
5	67,5	0,1	10	Argon	210,9	10,1
6	67,5	0,1	10	Nitrogen	208	6
7	67,5	0,1	15	Argon	211	11,2
8	67,5	0,1	15	Nitrogen	208	10
9	76,56	0,08	15	Argon	205,7	5
10	84,38	0,08	15	Argon	213,1	9,1
11	84,38	0,08	15	Nitrogen	204	5
12	135	0,05	10	Argon	209,4	8,3
13	135	0,05	10	Nitrogen	203	3
14	135	0,05	15	Argon	206,3	8,6
15	135	0,05	15	Nitrogen	200	16
Average					207,1	8,6

Table 2 - Hardness results according to different group samples

Thru Table 2, is possible to see that the average hardness values $207.1 \text{ Hv} \pm 8.6 \text{ Hv}$. The theoretical 316 L cast hardness value in 217 Hv. The samples produced by the commercial equipment achieved $267 \text{ Hv} \pm 19 \text{ Hv}$ (Figure 6).

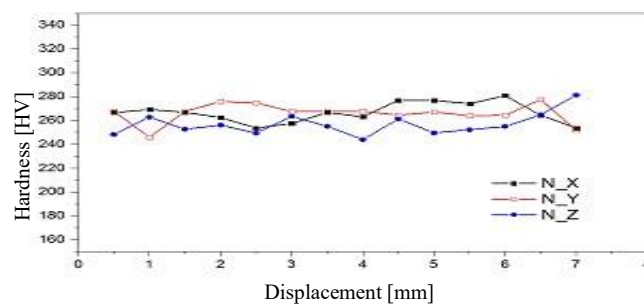


Figure 6 - Micro hardness test in the commercial equipment specimen faces perpendicular to X, Y and Z axis

The difference in hardness results may be related to the specimen grain size. It was possible to see in the metallographic images that the Concept Laser specimen have a grain size 2.5 times higher than the Adira specimens ($\sim 60 \mu\text{m}$).

The density measurement is a good indicator on the specimen building quality. The presence of porous will influence the mechanical properties, because it will work as a stress concentration point or a preferential path for crack growing. The presence of porous it will decreased the final piece density due to the increased on apparent volume.

It was used Archimedes density method and a Imaging (or Optic) method, to from the first technique understand the global porosity content of each specimen, and with the second technique, to see the porous size distribution and the possible origin. The Table 3 gather the Archimedes and Optic Relative density from the different 15 sample groups.

Specimen Group	Energy Density J/mm3	Hatch Spacing (mm)	Vector Size (mm)	Atmosphere	Rel. Density Archimedes (%)	Rel. Density Archi. Standard Deviation (%)	Rel. Density Optic (%)	Rel. Density Optic Standard Deviation (%)
1	67,5	0,1	1	Argon	99.4	0.01	99,769	0,194
2	67,5	0,1	1	Nitrogen	99.74	0.05	99,931	0,05
3	67,5	0,1	5	Argon	99.64	0.01	99,835	0,13
4	67,5	0,1	5	Nitrogen	99.10	0.02	99,88	0,121
5	67,5	0,1	10	Argon	99.19	0.01	99,783	0,193
6	67,5	0,1	10	Nitrogen	99.10	0.03	99,764	0,028
7	67,5	0,1	15	Argon	98.63	0.042	99,788	0,19
8	67,5	0,1	15	Nitrogen	98.8	0.21	99,838	0,112
9	76,56	0,08	15	Argon	99.1	0.5	99,722	0,129
10	84,38	0,08	15	Argon	99.00	0.56	99,785	0,102
11	84,38	0,08	15	Nitrogen	99.50	0.18	99,955	0,025
12	135	0,05	10	Argon	98.50	0.55	99,755	0,244
13	135	0,05	10	Nitrogen	98.63	0.2	99,996	0,105
14	135	0,05	15	Argon	99.00	0.54	99,752	0,24
15	135	0,05	15	Nitrogen	-	0.23	99,932	0,032
Average					99.10	0.21	99,83	0,13

Table 3 - Relative Density Results from the 15 groups experimental equipment samples.

Thru the Table 3 analysis, is possible to get the following tendencies:

- The Relative Density value increases with the increment in Volumetric Energy Input, as can be seen in the Figure 7 by the comparison between different energy input samples. This parameter gathers different parameters (ex: laser power, scan velocity, hatch space and vector size), allowing to generalized one variable with the general relative density content.

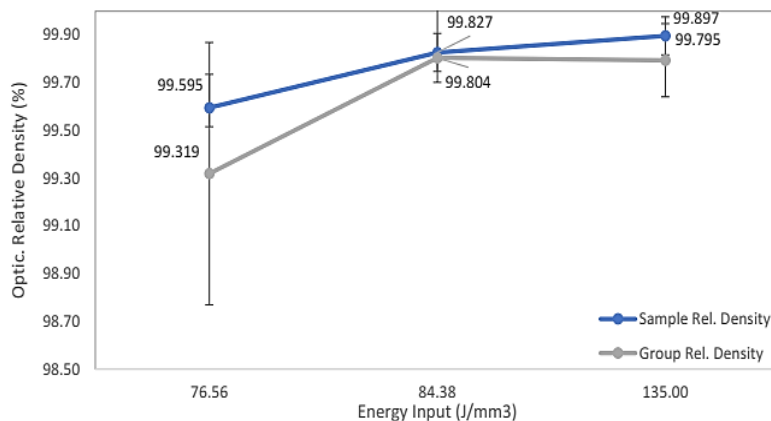


Figure 7 - Relative Density (%) Vs Energy Input (J/mm3). (Increasing the energy input by the hatch space parameter reduction), (9°, 10° and 14 Group Sample and representative sample from each group)

- The Relative Density decreases, with the increment in the vector size value, as can be seen in the Figure 8, mainly due to possible overheating in the scan line, that leads to a higher cooling time allowing the gas captation, however this phenomena needs a deeper study.

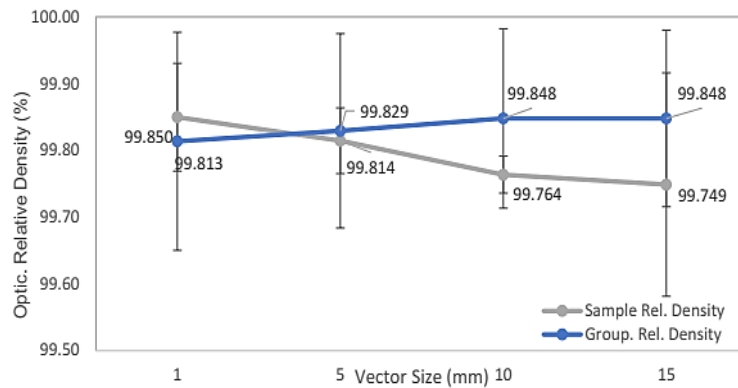


Figure 8 - Rel. Density (%) Vs Vector Size (mm), keeping the other variables constant (2°, 4°, 6° 8 Group Sample and representative sample from each group)

- The increment in hatch spacing leads to higher relative density values, as the Figure 11 shows. This result was not expected, accordingly with the bibliography, however because the standard deviation is higher than the variation of relative density between the different samples, this result needs a more in-depth study.

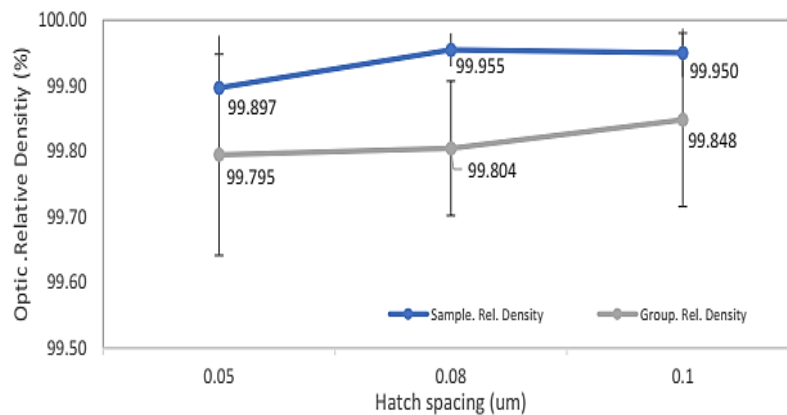


Figure 9 - Rel. Density (%) Vs Hatch Space (um), keeping the other variables constant (14°, 10° and 7° Group Sample and representative sample from each group)

- As the laser power is reduced, the energy input is decreased and the presence of defects as porosities as lack of fusion is increased.
- It was not noted any influenced, by now, from the protection atmosphere variation (Argon and Nitrogen).
- It is not observed a significant variation in the grain thickness (around 60 um)

If all the variables were, keep constant except the hatch distance and the vector size is possible to realize that:

- For the same vector size value, the specimens with lower hatch space values presented less porosities.
- For the same hatch distance value, the specimens with higher vector size presented higher porosities content

The lack of fusion porosity has a specific space distribution. The Figure 10 a) and b) show micrographs from the Z production axis, where is possible to see that the porosities are mainly located at the end of the scan line. This lack of fusion porosity comes from a shorter overposition laser scan, leading the powder that is between scan lines, not to be fully fused.

The Figure 10 c) and d) shows micrographs from the X production axis, where is possible to see that the porosity content is typical lower than in the Z production axis, and the porosities are located between powder layers.

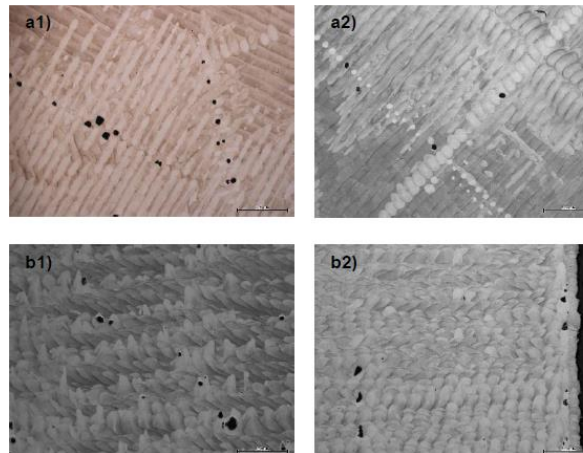


Figure 10 - Experimental Equipment specimens, Metallurgic images from: a1) and a2) in the Z axis; b1) and b2) in the X axis

To allow the mechanical behavior result comparison between the Adira and Concept Laser equipment, it was performed tensile tests in specimen produced by the commercial equipment and compressive tests in specimen produced by both equipments. The Figure 85 presents the compressive curves obtained, from specimens, of each equipment (Concept Laser and Adira).

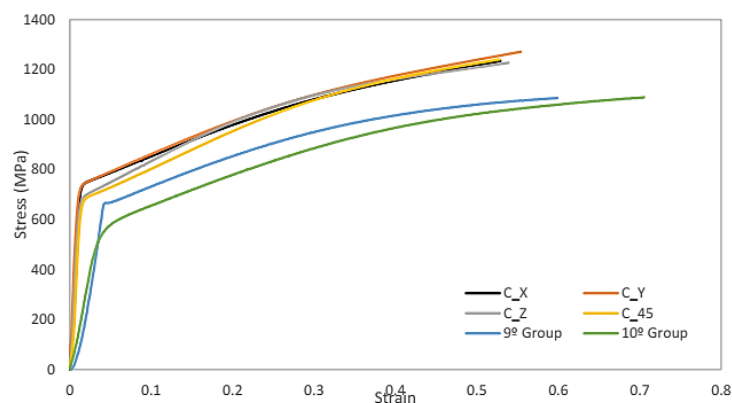


Figure 11 - Comparison between the average compressive stress and strain(True) curves between the commercial equipment specimens (C_X; C_Y; C_Z; C_45) and the experimental equipment specimens (9° and 10° group)

The results showed, that the Concept Laser specimens had a higher yield stress than Adira specimens, however all the samples showed a similar plastic mechanical behavior.

The compressive strength test, allows to identify that the samples with higher hardness values (Concept Laser), presented higher yield stress than Adira specimens that showed lower hardness values.

The Concept Laser specimens also presented a shorter resilience domain than the Adira specimen. These results can be related to the metallurgical grain size from each specimens. The Concept Laser specimens presented smaller grain sizes, leading typically to higher hardness values and more brittle mechanical behavior (smaller resilience domain). On the other hand, the Adira specimen presented higher grain size values, which leads to smaller hardness values and higher plastic deformation resistance (less brittle).

It was also performed, tensile tests in the Concept Laser samples in order to allow the comparison with a typical 316 L casted part (Table 4).

Sample	σ_{ced} (MPa)	σ_{ced} (Theoretical) (MPa)	ϵ_{ced}	σ_{UTS} (True) (MPa)	σ_{UTS} (Theoretical) (MPa)	ϵ_{UTS} (True)	$\sigma_{Rupture}$ (True) (MPa)	$\epsilon_{Rupture}$ (True)	E (GPa)	E (Theoretical) (GPa)
T-Y	643	172	0.0062	946	483	0.237	1018	0.476	103	193
T-X	653		0.0078	929		0.209	1229	0.548	84	
T-Z	580	-	0.0090	772	-	0.203	1240	0.768	65	
T-45	553	965	0.0085	826	1280	0.216	1120	0.637	65	

Table 4 - Stress and Strain values from tensile tests

Thru Table 4 is possible to identify that the specimen made in the building direction of 45° with all axis, has the lowest yield stress between all the specimens, being the T_Z with close yield stress values, these specimens (T_Z and T_45) showed lower UTS and rupture tension values.

This result may be related to, grain orientation in the solidification phase presenting a preferential deformation path, decreasing the resistance to crack propagation.

Table 4 shows a lower Young modulus for the T_Z and T_45 samples being the Young modulus obtained from the tensile curve slope in the linear section.

4. Conclusions

The experiments had the purpose to develop the Adira SLM equipment (Addcreator) and to understand how the different set parameter related between each other.

One interesting result was the influence on the vector length and the hatch distance in the density part. Where it was possible to notice that, a small vector length and hatch distance values, leads to greater volumetric energy input that is required to melt the powder material, and to achieve the smallest porosity content possible.

Another porosity related conclusion, is the porosity heterogenic position along the specimen, where it was possible to see that the porosity content is greater in the specimen periphery. However, this outer region can be erased by polishing the surface.

Porosity origin from lack of fusion, is mainly in the end of the scan line in the Z direction. This surface porosity content needs time to understand the porosity origin and how these phenomena can be reduced.

The density results, show generally the same tendency for the group specimens and representative samples. The Archimedes density method allows to identify that the Adira equipment manufacture specimens with relative density values higher than 99%. However, the standard deviation is higher than the difference in the Relative density result values between the specimens under analysis.

The experiments also show, a final layer oxidation problem in the experimental equipment, due to the entrapped air between the powders that is released to the laser chamber atmosphere promoting the surface oxidation. This problem was noted in the Concept Laser and in the Adira equipment.

The compressive tests allowed to identify, the relation between the grain size, hardness values and the mechanical resistance. Adira samples presented a higher resilience domain but have lower yield stress than Concept Laser specimens.

This thesis allows to validate, the specimens produced by the Adira equipment, concluding that Adira specimen has presented closest properties to the cast 316L parts, than the specimen manufactured from Concept Laser equipment.

This thesis permitted, to go further in the influence of manufactured conditions in the final mechanical properties. In respect of manufactured conditions, it was possible to study the impact on each process parameter.

References

- [1] J. & H. & S. M. & N. Lavery, “Investigation into the effect of process parameters on microstructural and physic: properties of 316L stainless steel parts by selective laser melting,” *Journal Adv Manuf Technol*, pp. 869 - 979, 2011.